22NM NODE P+ USJ USING XE-PAI & LASER ANNEALING

John Borland
J.O.B. Technologies, 98-1204 Kuawa St., Aiea, Hawaii, 96701

Zhimin Wan
AIBT, 81 Daggett Dr., San Jose, CA 95134

Shankar Muthukrishnan and Jeremy Zelenko
Applied Materials, Inc., 974 E. Arques, Ave., Sunnyvale, CA 94085

Iad Mirshad and Walt Johnson
KLA-Tencor, 160 Rio Robles Rd., San Jose, CA 95134

Temel Buyuklimanli
EAG, 104 Windsor Center Dr., Suite 101, East Windsor, NJ, 08520

We investigated 100eV B and 500eV BF_2 implants to achieve very aggressive shallow p+ USJ 6-10nm deep. To maximize dopant activation with minimal diffusion we used laser annealing at 4 different temperatures (1175C, 1225C, 1275C and 1325C). No channeling was observed for monomer B at 100eV but to enhance dopant activation with laser annealing both Ge-PAI and Xe-PAI were used. The highest dopant activation was achieved with the 1325C laser anneal and as expected Ge-PAI improved Rs for monomer B from 1700ohms/sq (Bss=1E20/cm^3) to 900ohms/sq (Bss=1.3E20/cm^3), however, Xe-PAI was best at 380ohms/sq (Bss=3.5E20/cm^3). For BF_2 the Rs dopant activation values were about 2x worse than monomer B. We also observed characterization metrology of shallow junctions below 12nm can be erroneous depending on the junction leakage quality.

INTRODUCTION

32nm node high performance logic production starts by the end of 2009 and the 22nm node 2 years later in 2011. The target junction depth (Xj) for 22nm node p+ USJ is 6-10nm after annealing. Borland reported back in 2006 that this would require B<100eV or BF_2<500eV implant energy without channeling and energy contamination (1). At this technology node diffusion-less annealing will be necessary so MSA (msec anneal) only or MSA+<900C spike/RTA is required to realize high quality USJ with stable defects as reported by Borland & Kiyama at IIT-2008 (2). Using PAI (pre-amorphizing implant) eliminates B channeling and with MSA enhances dopant activation to the 1-2E20/cm^3 boron solid solubility (Bss) level. But minimal dopant diffusion and the residual EOR (end of range) damage can lead to junction leakage degradation requiring higher MSA temperature >1300C or <900C diffusion-less spike/RTA anneal for defect stability (3). Also, different PAI species leads to different levels of residual implant damage. Matsuda reported less residual PAI damage and lower junction leakage when using Ge-PAI compared to Si-PAI with SPE annealing (4). Higher atomic mass PAI species improves amorphous layer interface and lowers the critical dose for amorphization with less residual implant damage and EOR defect after annealing. With In-PAI at <5E13/cm^2 dose, after MSA there is no residual EOR damage as reported by Sawada et al. at SSDM-2008 (5) and no degradation in junction leakage as reported by Borland & Kiyama (2). Therefore we investigated Xe species as an alternative for PAI due to its inert

chemical nature compared to Ge or In, not forming substitutional sites and thereby not inducing any strain-Si effects (compressive nor tensile) for p+ USJ at 22nm node.

EXPERIMENTATION

The AIBT iPulsar implanter was used with its unique S-bend beam-line design to minimize energy contamination to <0.1% when using >10 to 1 decel ratio (6). B 100eV/1e15/cm^2 dose and BF_2 500eV/1E15/cm^2 dose were implanted into n-type 300mm wafers at a decel ratio of 70 to 1. To reduce channeling effects some wafers had Ge-PAI 10keV at 1 & 5E14/cm^2 and Xe-PAI 14keV at 1 & 0.5E14/cm^2. To compare the effects of MSA temperature on dopant activation and defect stability the Applied DSA scan laser annealer was used to anneal 4 different temperature zones per wafer at 1175C, 1225C, 1275C and 1325C without capping layer as shown in Fig.1 which is a thermal-wave (TW) full wafer map image of wafer #14 after DSA laser annealing showing the 4 different annealing regions.

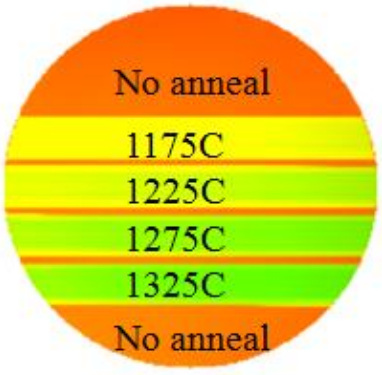

Fig.1: Thermal-wave full wafer image mapping showing the 4 different laser annealing temperature zones created by the DSA laser scan.

RESULTS

A summary of the results for the various implants and annealing conditions are shown in Table I. We first did RsL sheet resistance (Rs) and junction leakage measurements at Frontier Semiconductor. Both full wafer maps and diameter line scans were done on all the wafers as represented by the data in Fig. 2 for the Ge+B wafer #15. If the junction was very leaky >2.5E-2A/cm^2 no Rs value could be calculated as shown in Fig.3 for wafer #17 (Xe+B) and listed as “leaky” junctions in Table I. The plot of RsL junction leakage is shown in Fig.4 and sheet resistance in Fig.5. As expected the higher the laser annealing temperature the lower the junction leakage current and better the dopant activation (Rs) so the 1325C results were best compared to lower temperature anneals.

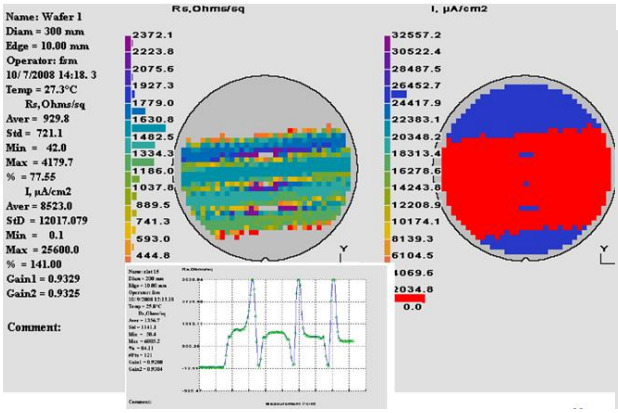

Fig.2: RsL results for Ge+B wafer #15.

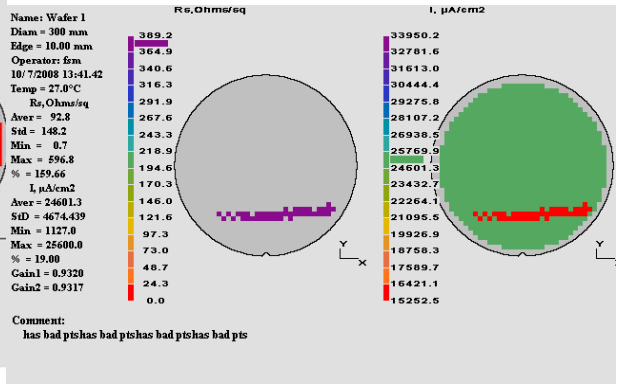

Fig.3: RsL results for Xe+B wafer #17.

Table I: p+ USJ Implant Matrix & Results

Request	Sequence	Recipe	Wafer slot		No DSA	1175C	1225C	1275C	1325C
1	1	B-100eV-1E15	14	Rs (Hz probe)	9000	5000	3000	2300	1800
				Rs	6500	3600	3600	2600	1700
				JL(A/cm2)	1.30E-05	6.00E-06	<1E-6	<1E-6	<1E-6
				Thermal-wave	1984	1336	1233	1135	1085
2	1	Ge-10keV-5E14	15	Rs (Hz probe)	30	890	1100	1200	1215
	2	B-100eV-1E15		Rs	Leaky!	1800	1500	1350	900
				JL(A/cm2)	Leaky!	<2E-3	<2E-3	<2E-3	<2E-3
				Thermal-wave	13,834	2490	2052	1666	1385
3	1	Ge-10keV-1E14	16	Rs (Hz probe)	30	1450	1800	1500	1300
	2	B-100eV-1E15		Rs	Leaky!	2500	2000	1600	1000
				JL(A/cm2)	Leaky!	<2E-3	<2E-3	<2E-3	<2E-3
				Thermal-wave	7059	2356	1749	1324	1235
4	1	Xe-14keV-1E14	17	Rs (Hz probe)	47	64	242	597	725
	2	B-100eV-1E15		Rs	Leaky!	Leaky!	Leaky!	Leaky!	380
				JL(A/cm2)	Leaky!	Leaky!	Leaky!	Leaky!	1.50E-02
				Thermal-wave	11,267	3488	3451	3375	3296
4		**Post 875C**	18	Rs (Hz probe)	1025	1150	1200	925	775
	1	Xe-14keV-1E14		Rs	900	733	690	653	572
	2	B-100eV-1E15		JL(A/cm2)	<1E-7	<1E-7	<1E-7	<1E-7	<1E-7
				Thermal-wave	3305	3393	3402	3402	3380
5	1	Xe-14keV-5E13	19	Rs (Hz probe)	30	78	325	500	575
	2	B-100eV-1E15		Rs	Leaky!	Leaky!	Leaky!	560	601
				JL(A/cm2)	Leaky!	Leaky!	Leaky!	<4E-3	<4E-3
				Thermal-wave	8797	3364	3341	3257	3155
6	1	BF2-500eV-1E15	20	Rs (Hz probe)	6000	4300	3300	2700	2400
				Rs	26,000	8800	6600	4400	4400
				JL(A/cm2)	<1E-7	<1E-7	<1E-7	<1E-7	<1E-7
				Thermal-wave	2006	1117	1103	1095	1106
7	1	Ge-10keV-5E14	21	Rs (Hz probe)	30	1000	1450	1515	1520
	2	BF2-500eV-1E15		Rs	Leaky!	2000	2000	1800	1400
				JL(A/cm2)	Leaky!	<2E-3	<2E-3	<2E-3	<2E-3
				Thermal-wave	13,714	2492	2037	1725	1491
8	1	Ge-10keV-1E14	22	Rs (Hz probe)	33	1500	2000	1800	1700
	2	BF2-500eV-1E15		Rs	Leaky!	2500	2300	2000	1400
				JL(A/cm2)	Leaky!	<2E-3	<2E-3	<2E-3	<2E-3
				Thermal-wave	7102	2294	1653	1315	1299
9	1	Xe-14keV-1E14	23	Rs (Hz probe)	33	35	100	300	450
	2	BF2-500eV-1E15		Rs	Leaky!	Leaky!	Leaky!	Leaky!	Leaky!
				JL(A/cm2)	Leaky!	Leaky!	Leaky!	Leaky!	Leaky!
				Thermal-wave	11,237	3463	3439	3375	3322
		Post 875C		Rs (Hz probe)	1600	1600	1800	1500	1212
9	1	Xe-14keV-1E14	24	Rs	1407	1030	967	967	904
	2	BF2-500eV-1E15		JL(A/cm2)	1.00E-06	<1E-7	<1E-7	<1E-7	<1E-7
				Thermal-wave	3199	3338	3337	3346	3351
10	1	Xe-14keV-5E13	25	Rs (Hz probe)	32	60	225	600	900
	2	BF2-500eV-1E15		Rs	Leaky!	Leaky!	Leaky!	Leaky!	460
				JL(A/cm2)	Leaky!	Leaky!	Leaky!	Leaky!	<1.3E-2
				Thermal-wave	8839	3330	3326	3272	3215

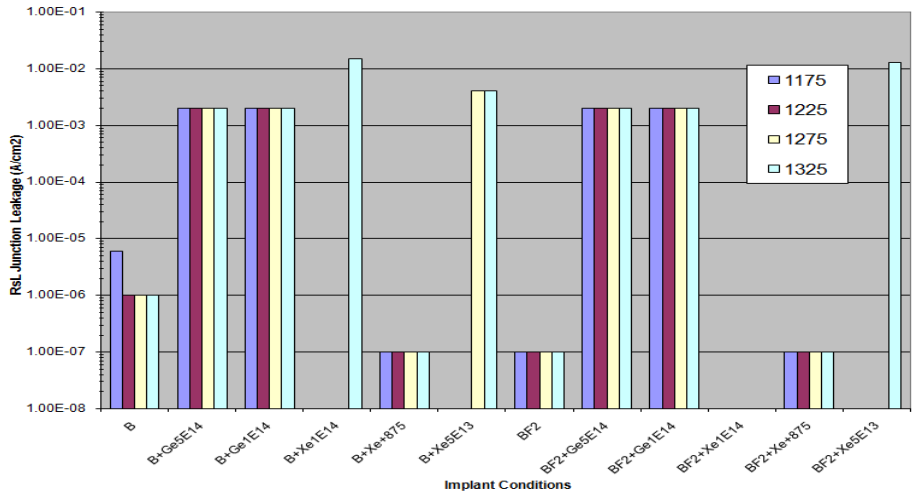

Fig.4: RsL junction leakage results.

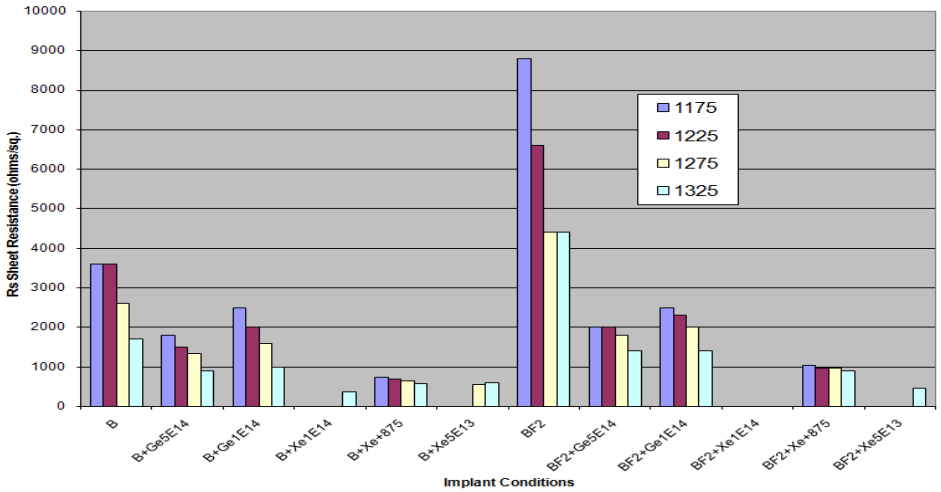

Fig.5: RsL sheet resistance results.

To get an Rs value for even the leaky junctions caused by the PAI end of range damage, KLA-Tencor used their Rs-200 4PP with special flat probe tips (Hx-probes). The 4PP Rs results including the leaky junctions are shown in Fig.6 and listed in Table I. On "leaky" junctions we observed the opposite Rs trend with 4PP, lower Rs at lower temperatures. Rs values of ~30 ohms/sq. were measured for the no anneal regions for all the wafers and increased with annealing temperature up to 1325C as measured on wafers #15, 17, 19, 21, 23 & 25 shown in Table I & Fig. 6 so 4PP does not give accurate Rs values on leaky junctions. Note the no annealed region has an Rs value of 47 ohms/sq. which would be the n-type substrate Rs value. These erroneous low Rs values were not observed with RsL sheet resistance measurement in Table I because RsL first checks for junction leakage before calculating Rs value. Using a special software program on the 4PP system a test for junction leakage was conducted and the results are shown in Fig.7 for the leaky junctions in wafer #17 and Fig.8 for the low leakage junctions in wafer #18 which had an additional 875C furnace anneal which diffused the junction deeper to 44-55nm. With leaky junctions, increasing the 4PP measurement current reduces the sheet resistance for the junctions by 15% as shown for wafer #17 in Fig.7 while the 4PP Rs values stayed constant for the low leakage junctions for wafer #18 in Fig.8. Therefore, if the junction is leaky, 4PP measured Rs values can be in error.

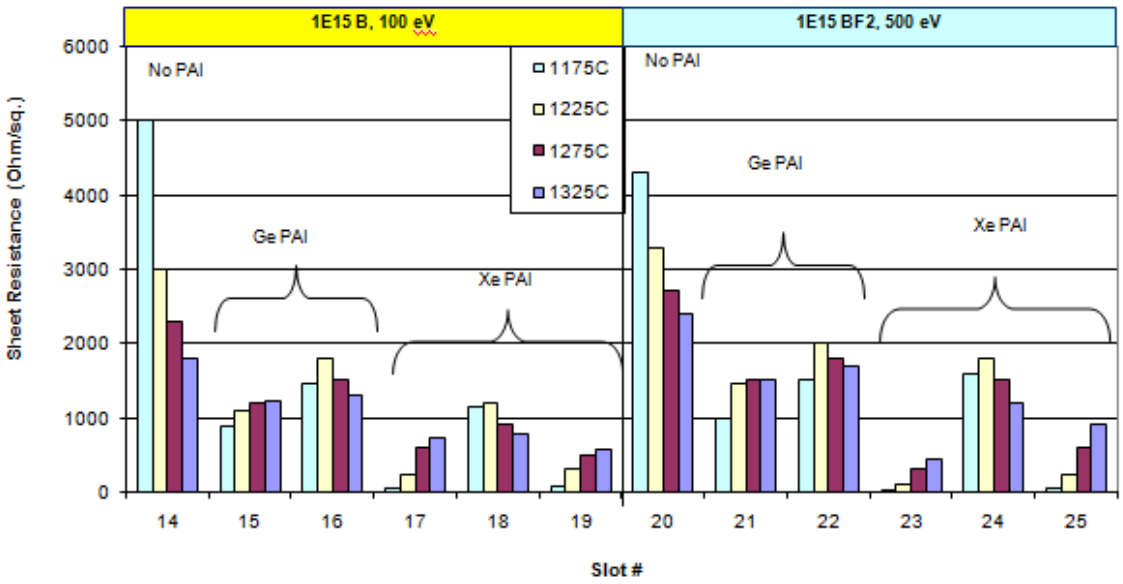

Fig.6: 4PP sheet resistance using Hx probes.

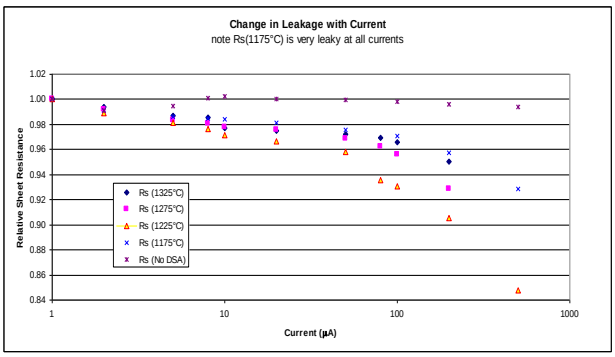

Fig.7: Wafer #17 4PP leaky junction.

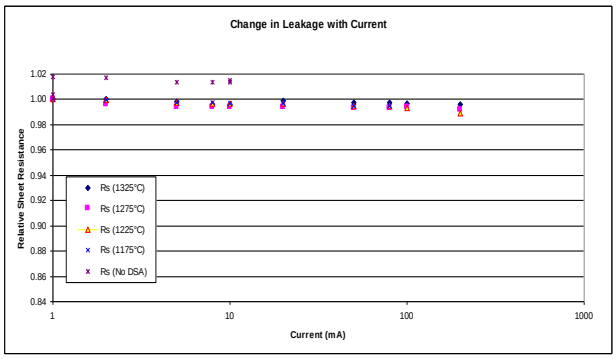

Fig.8: Wafer #18 4PP low leakage junction.

The thermal-wave (TW) results comparing wafers #17 & 18 are shown in Figs. 9 & 10. A 5.6mm periodic stepping pattern can clearly be detected in wafer #17 but in wafer #18 which had the additional 875C furnace anneal the pattern could not be seen for the lower 1175C and 1225C laser temperatures and reduced on the higher 1275C and 1325C annealed regions. The disappearance in the TW signal valleys between scan locations with the 875C post anneal may be an indicator of improved leakage. As expected higher MSA temperature results in lower residual implant damage as detected by TW for the B wafers #14, 15, 16, 17 & 19 as shown in Fig.11 and BF_2 wafers #20, 21, 23 & 25 in Fig.12. With the 875C furnace anneal, the TW values showed no significant temperature dependence for the Xe-PAI wafers.

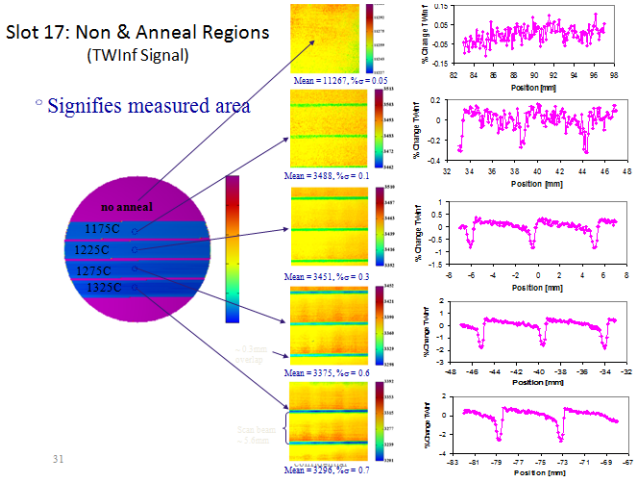

Fig.9: Wafer #17 thermal-wave wafer map.

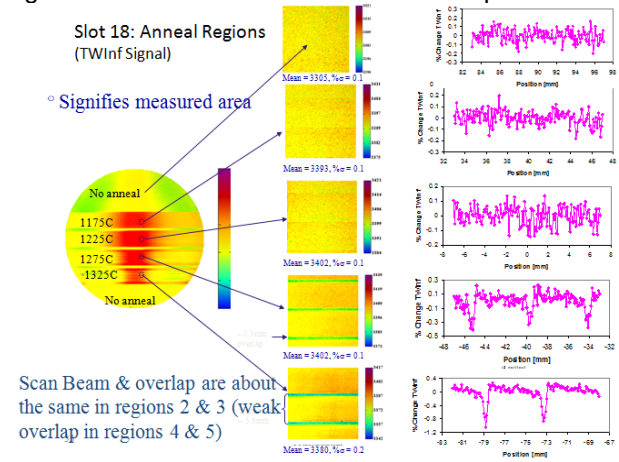

Fig.10: Wafer #18 thermal-wave wafer map.

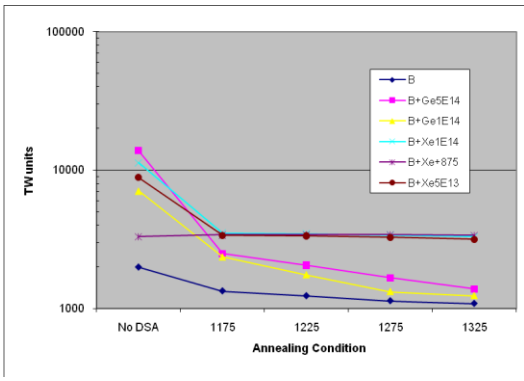

Fig.11: B implanted wafers TW results.

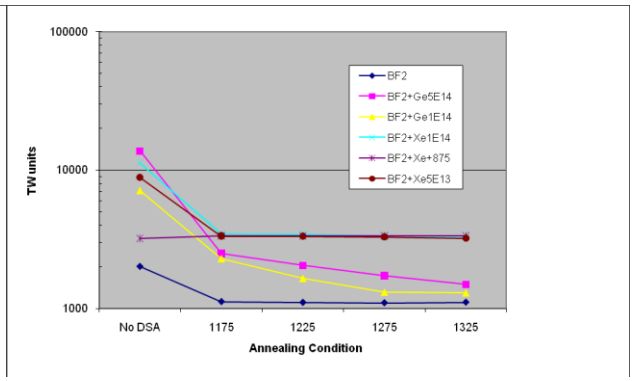

Fig.12: BF_2 implanted wafers TW results.

X-TEM results for wafer #17 (Xe-PAI+B) is shown in Fig. 13 for the no anneal and 1325C anneal regions. The 14keV/1E14/cm^2 Xe-PAI implant results in a 14nm deep amorphous layer and after the 1325C laser anneal no evidence of residual implant damage nor EOR defects could be observed in agreement with the TW results in Fig.11, but RsL leakage results showed the junction still to be leaky. A 2.3nm thick surface oxide was also detected by X-TEM in Fig.13 and this could be due to the fact that after implant the wafers were subjected to several full wafer metrology techniques for 5 months prior to wafer breakage for X-TEM and SIMS analysis. SIMS analysis was performed by Evans Analytical Group (EAG) using a new technique (PCOR-SIMS^{SM}) capable of detecting surface oxide and accurate near surface shallow profiles. The SIMS profiles are shown in Fig. 14a and in agreement with the X-TEM results the surface oxide was determined to be about 2.3nm thick. We also determined that 48-63% of the boron dose was in the oxide layer as shown in Table II. EAG also used XPS to determine the oxide thickness and BIC (boron interstitial cluster) concentration shown in Table II. They also performed an HF-dip on wafer #14 to remove the surface oxide and the after HF-dip SIMS plot is shown in Fig.14b for the 1325C annealed region of wafer#14 with an Xj=7.2nm. Using the corrected SIMS Xj by subtracting the surface oxide thickness and using Rs values from RsL we determined the Bss (boron solid solubility) values from the Rs/Xj plot shown in Fig.15. For the 1325C laser anneal temperature B without PAI Bss=1E20/cm^3, Ge-PAI+B Bss=1.3E20/cm^3 and Xe-PAI+B Bss=3.5E20/cm^3. This agrees with the estimated Bss level from the B SIMS profiles in Fig. 14a which for Xe+B~4E20/cm3, Ge+B~2.5E20/cm^3 and B~2E20/cm^3. We also had CAOT (continuous anodic oxidation technique) performed at UCLA but had difficulties with these shallow junctions. For the deep 875C annealed junction CAOT measured Bss~5E19/cm^3 in agreement with Fig. 15 showing Bss=4E19/cm^3. CAOT also detected a drop in mobility at 4nm depth.

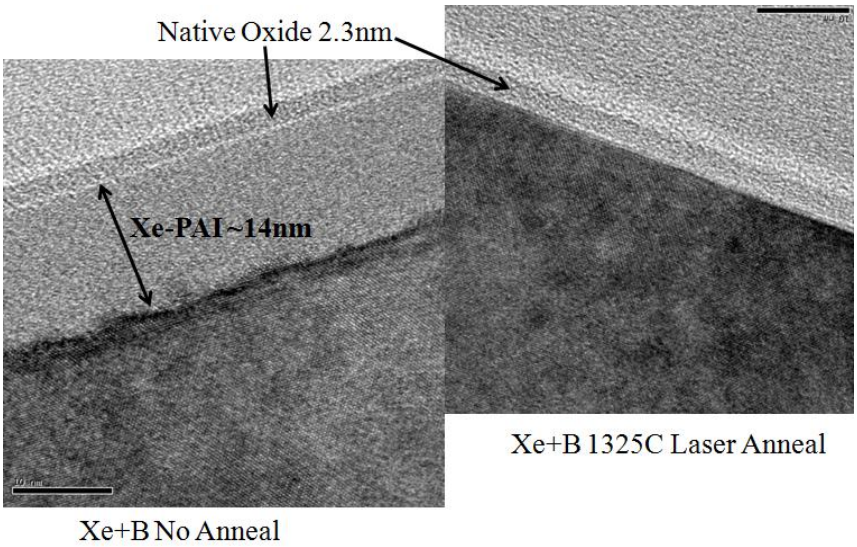

Fig.13: X-TEM analysis of wafer #17 (Xe-PAI+B) no anneal and 1325C anneal regions.

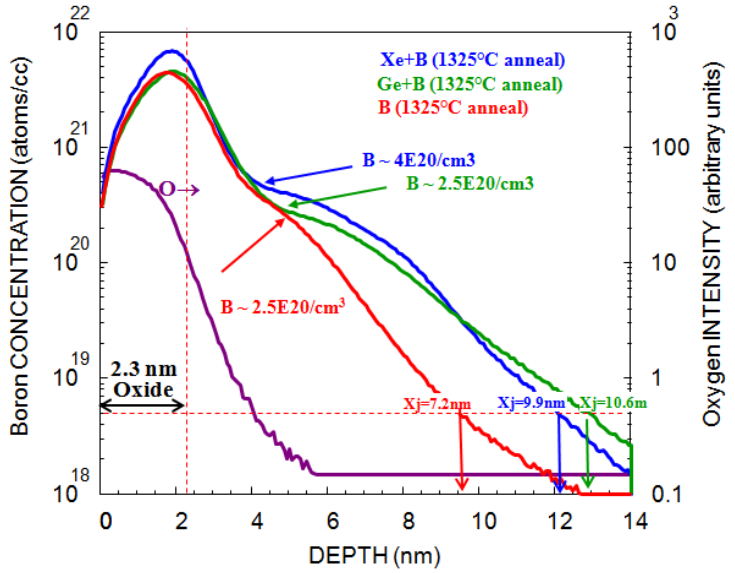

a)

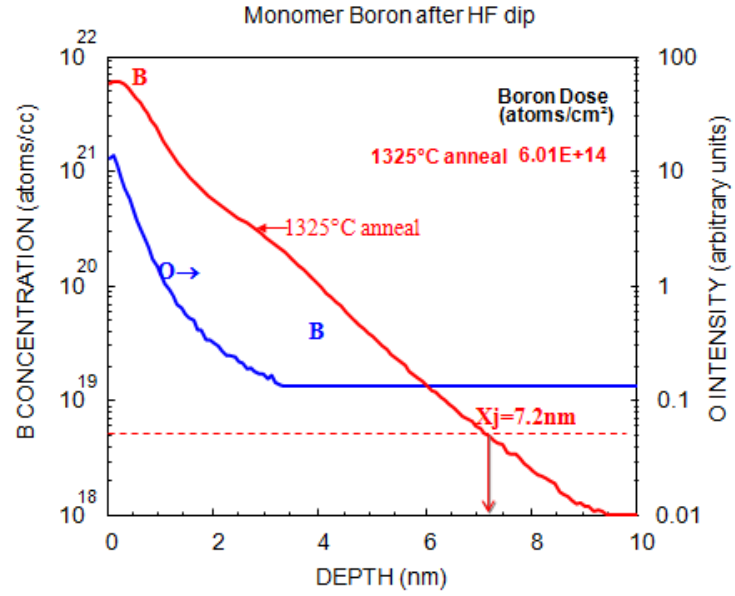

b)

Fig.14: PCOR-SIMS[SM] analysis results showing a) 2.3nm of surface native oxide and b) after HF-dip to remove 2.3nm of surface oxide showing Xj=7.2nm after 1325C anneal.

Table II: SIMS & XPS Results

Sample ID	Dose in oxide (atoms/cm²)	Total dose (Si+oxide) (atoms/cm²)	Oxide/total Dose ratio	Xj (nm) @ 5E18at/cc	t_{ox} (nm)	BIC (atoms/cc)	B-(Si_4), SiB_x (atoms/cc)
Wafer #14 (1325C anneal)	6.32E+14	9.97E+14	63%	8.6	2.24	-	1.70E+21
Wafer #15 (1325C anneal)	5.17E+14	9.93E+14	52%	12.9	2.3	-	1.80E+21
Wafer #17 (1325C anneal)	7.76E+14	1.33E+15	58%	12.1	2.23	-	2.80E+21
Wafer #18 (1325C anneal + 875C furnace)	5.85E+14	1.22E+15	48%	57.5	2.32	-	2.50E+21
Wafer #14 (no anneal)	5.73E+14	9.50E+14	60%	8.4	2.33	2.80E+20	6.10E+20
Wafer #15 (no anneal)	4.85E+14	9.46E+14	51%	9.0	2.37	8.20E+20	1.60E+21
Wafer #17 (no anneal)	6.87E+14	1.23E+15	56%	9.0	2.21	6.20E+20	2.50E+21
Wafer #18 (875C furnace only)	5.68E+14	1.17E+15	49%	44.7	2.38	-	3.30E+21

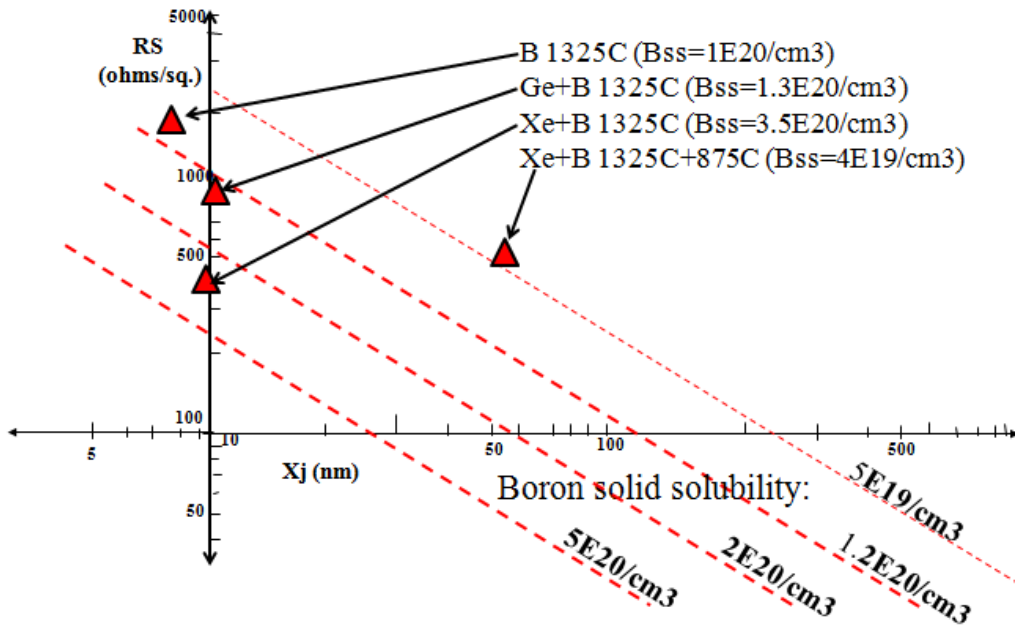

Fig.15: RsL sheet resistance versus SIMS Xj for the 1325C laser anneal.

SUMMARY

Monomer B implantation at 100eV/1E15/cm2 dose showed no channeling with an Xj~6.5nm. A 1325C laser anneal resulted in 0.7nm of diffusion but with Ge-PAI or Xe-PAI the diffusion was 3.9nm and 3.1nm respectively. The highest dopant activation at 1325C was with Xe-PAI (Bss=3.5E20/cm^3) compared to Ge-PAI (Bss=1.3E20/cm^3) and no PAI (Bss=1E20/cm^3). To avoid erroneous 4PP Rs values even with flat Hx-probes, check for junction leakage prior to trusting an Rs value. PCOR-SIMS^{SM} analysis detected the thickness of the surface oxide so corrected junction depths could be accurately determined compared to conventional SIMS analysis with O_2-flooding or normal incidence impact which could not distinguish the surface oxide effects which is important for process and device simulation models especially for shallow junctions <10nm deep. Thermal-wave was used to detect residual implant damage and we had difficulties with CAOT measurements on these shallow junctions.

ACKNOWLEDGEMENTS

The authors are grateful to David Lu of Frontier Semiconductor for the 875C anneals and the RsL measurements. Also to Si Prussin of UCLA for the CAOT measurements and Kevin Jones of the University of Florida for quick X-TEM turn around.

REFERENCES

1) J. Borland, Semiconductor International, Dec. 2006, p. 49.
2) J. Borland and H. Kiyama, IIT-2008, June 2008, p. 63.
3) J. Borland, IWJT-2008, p. 68.
4) T. Matsuda, Semicon/Japan vTech 2002, Dec. 2002 presentation material.
5) T. Sawada et al., SSDM-2008, Sept. 2008, paper B-8-4.
6) C. Jen, Semicon/Taiwan Sept. 2008 AIBT implant seminar presentation material.